

Metal Oxide Chemistry in Solution: The Early Transition Metal Polyoxoanions

Victor W. Day and Walter G. Klemperer

Summary. Many of the early transition elements form large polynuclear metal-oxygen anions containing up to 200 atoms or more. Although these polyoxoanions have been investigated for more than a century, detailed studies of structure and reactivity were not possible until the development of modern x-ray crystallographic and nuclear magnetic resonance spectroscopic techniques. Systematic studies of small polyoxoanions in inert, aprotic solvents have clarified many of the principles governing their structure and reactivity, and also have made possible the preparation of entirely new types of covalent derivatives such as $\text{CH}_2\text{Mo}_4\text{O}_{15}\text{H}^{3-}$, $\text{C}_5\text{H}_5\text{TiMo}_5\text{O}_{18}^{3-}$, and $(\text{OC})_3\text{Mn}(\text{Nb}_2\text{W}_4\text{O}_{19})^{3-}$. Since most early transition metal polyoxoanions have structures based on close-packed oxygen arrays containing interstitial metal centers, their chemistry offers a rare opportunity to study chemical transformations in detail on well-defined metal oxide surfaces.

Inorganic chemists have been attracted to the aqueous solution chemistry of the early transition metals vanadium, niobium, tantalum, molybdenum, and tungsten since the mid-19th century, when it was discovered that these elements, in their highest oxidation states, easily form large, polynuclear oxoanions $\text{M}_x\text{O}_y^{z-}$, where $\text{M} = \text{V}^{\text{V}}, \text{Nb}^{\text{V}}, \text{Ta}^{\text{V}}, \text{Mo}^{\text{VI}},$ or W^{VI} (1, 2). A wide variety of discrete, molecular ions, ranging in complexity from relatively small species such as $\text{V}_2\text{O}_7^{4-}$ to larger analogs such as $\text{Mo}_{36}\text{O}_{128}\text{H}_{32}^{8-}$, may be obtained from aqueous solutions at different pH values (1). The reaction chemistry of early transition metal polyoxoanions has traditionally been restricted to Brønsted acid-base transformations. The $\text{P}_2\text{Mo}_5\text{O}_{23}^{6-}$ ion, for example, is prepared in aqueous solution as an NH_4^+ salt from H_3PO_4 , $(\text{NH}_4)_6\text{Mo}_7\text{O}_{24}$, and NH_4OH (2). Related organic derivatives such as $(\text{CH}_3)_2\text{AsMo}_4\text{O}_{15}\text{H}^{2-}$ have been prepared in a similar fashion, here from addition of MoO_3 to aqueous $(\text{CH}_3)_2\text{AsO}_2\text{H}$ plus NaOH (3).

During the past decade, there has been a resurgence of interest in the chemistry of early transition metal polyoxoanions, prompted principally by three independent developments. First, analytical instrumentation has reached the point of technological sophistication where extremely complex inorganic species can be structurally characterized on a routine basis by using x-ray diffraction in the solid state and nuclear magnetic resonance (NMR) spectroscopy in the solution state. The resulting structural information has clarified some of the relationships between structure, bonding, and reactivity and enabled chemists to approach these systems in a fairly rational fashion. A second key development has been the expansion of synthetic methodology beyond Brønsted acid-base chemistry

to more general types of covalent transformations of the type traditionally employed in organic and organometallic chemistry. This expansion is largely a consequence of the availability of reactive polyoxoanions having organic counterions such as tetraalkylammonium cations that solubilize them in nonaqueous, organic solvents well suited for organic and organometallic reaction chemistry. The final development responsible for renewed interest in polyoxoanion chemistry, a development not discussed in this article, is the industrial application of early transition metal polyoxoanions as catalysts for the selective air oxidation of organic molecules (4). This development has not only expanded research activities in the industrial community but has also alerted academic researchers to previously unanticipated modes of reaction chemistry.

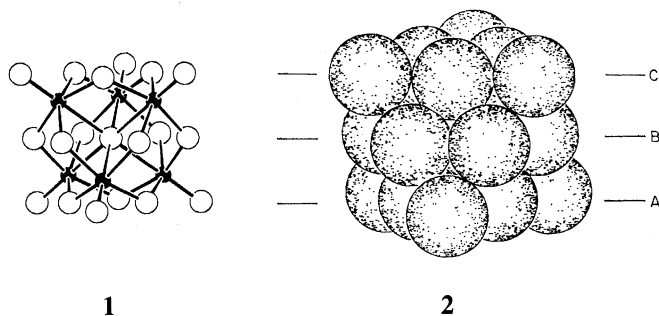
Background

An obvious feature of the early transition metal polyoxoanions is their unusually large size, a feature which places their solution chemistry in a region intermediate between small molecule solution chemistry and infinite lattice solid-state chemistry. The relationship between polyoxoanions and solid oxides extends beyond simple size considerations, however, to more subtle aspects of structure and bonding. These relationships are perceived most clearly through a detailed examination of two simple but representative polyoxoanions, $\text{W}_6\text{O}_{19}^{2-}$ and $\text{CH}_2\text{Mo}_4\text{O}_{15}\text{H}^{3-}$.

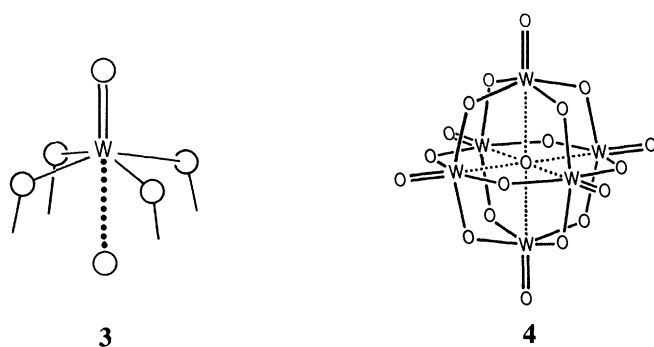
The structure of the octahedral $\text{W}_6\text{O}_{19}^{2-}$ anion (5) is shown in **1** as a ball-and-stick model where small, filled circles represent tungsten centers; large open circles represent oxygen centers; and lines represent tungsten-oxygen bonds. The same structure is shown in **2** as a space-filling model where oxygen centers are drawn as shaded spheres having van der Waals radii (1.4 Å). This model shows how the oxygens in

Victor W. Day is an associate professor of chemistry at the University of Nebraska, Lincoln 68588. Walter G. Klemperer is a professor in the Department of Chemistry and a member of the Materials Research Laboratory at the University of Illinois at Urbana-Champaign, Urbana 61801.

$W_6O_{19}^{2-}$ form three close-packed layers and how these layers are arranged in a cubic close-packed (ABC) fashion. Inspection of **1** reveals the location of the metal centers in the octahedral interstices between the oxygen atoms. The $W_6O_{19}^{2-}$ structure is thus a fragment of the NaCl lattice structure, whose metal centers occupy octahedral interstices in a cubic close-packed chloride array.



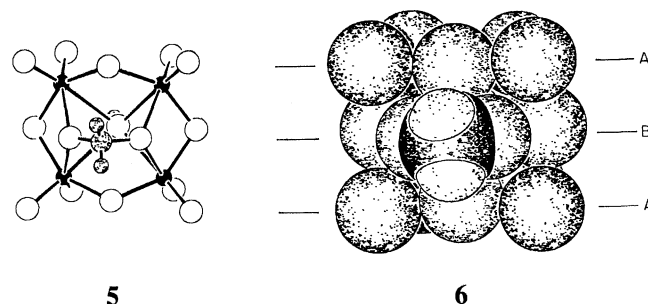
Since the tungsten atoms in $W_6O_{19}^{2-}$ are in their highest oxidation state (+6), there are no tungsten valence electrons available for metal-metal bonding, and the structure is held together only by the metal-oxygen bonds shown in **1**. Closer examination of this structure reveals three different types of metal-oxygen bonds at each tungsten center (see **3**). Each tungsten center forms one very short (1.69 Å) bond to a terminally bonded OW oxygen which corresponds to a double bond, four somewhat longer (1.92 Å) bonds to doubly bridging OW_2 oxygens which correspond to single bonds, and finally a very long and weak bond (2.33 Å) to the central, sixfold bridging OW_6 oxygen atom represented by the dotted line in **3** (5, 6). Hexavalence at tungsten is thus seen to be satisfied, to a first approximation, by the formation of one double bond and four single bonds to oxygen centers. When the individual units shown in **3** are linked together to form the $W_6O_{19}^{2-}$ structure (see **4**), the structure appears as a neutral W_6O_{18} cage encapsulating an O^{2-} anion, that is, $[(W_6O_{18})(O^{2-})]$.



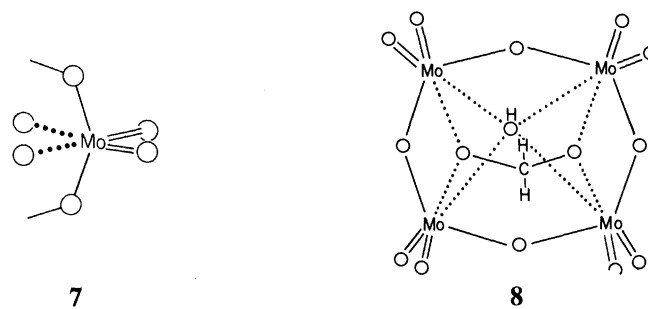
From this viewpoint, many other W^{VI} and Mo^{VI} polyoxoanions (*I*) are seen to be based on larger, neutral W_nO_{3n} cages that encapsulate anionic subunits and are linked to them only by very weak, >2.2 Å bonds; $PMo_{12}O_{40}^{3-}$ contains an $Mo_{12}O_{36}$ cage encapsulating a phosphate ion, $[(Mo_{12}O_{36})(PO_4^{3-})]$; $W_{10}O_{32}^{4-}$ contains a $W_{10}O_{30}$ cage encapsulating two oxide ions, $[(W_{10}O_{30})(O^{2-})_2]$; $P_2Mo_{18}O_{62}^{6-}$ contains an $Mo_{18}O_{54}$ cage encapsulating two phosphate ions, $[(Mo_{18}O_{54})(PO_4^{3-})_2]$; and so on. In the limit of an infinitely large cage formed by linking type **3** units, an infinite sheet structure is formed. Precisely such sheets are found in the $MoO_3 \cdot 2H_2O$ structure (**7**). Here, each Mo^{VI} forms a double bond to a terminal OMo oxygen, four single bonds to bridging OMo_2 oxygens, and one very weak bond to a water oxygen.

The second water lies between the $MoO_3 \cdot H_2O$ layers and is not bonded to molybdenum.

The $CH_2Mo_4O_{15}H^{3-}$ anion (**8**) represents a different class of polyoxoanion structures. The geometry of this C_{2v} symmetry species is shown in **5**, where open circles represent oxygen atoms, filled circles represent molybdenum atoms, small shaded circles represent hydrogen atoms, and the large shaded circle represents the carbon atom. The space-filling representation **6** reveals a close-packed arrangement of oxygens,



here three layers arranged in a hexagonal close-packed (ABA) fashion. Since the metals occupy octahedral holes in this oxygen array, the Mo_4O_{15} core of the $CH_2Mo_4O_{15}H^{3-}$ anion is seen to be a fragment of the NiAs lattice structure, where metal centers occupy all the octahedral holes in an hexagonal close-packed arsenic array. Bonding at each of the hexavalent molybdenum centers in the anion (see **7**) involves formation of double bonds to each of two terminal O_2Mo oxygens, single bonds to each of two doubly bridging OMo oxygens, and very weak bonds to the centrally located $OCMo_2$ and $OHMo_4$ oxygens. By linking such units together to form the complete valence structure **8**, the $CH_2Mo_5O_{15}H^{3-}$ anion is seen to



consist of OH^- and $CH_2O_2^{2-}$ units linked by weak bonds to opposite sides of an Mo_4O_{12} ring and can be conveniently represented by the formula $[(Mo_4O_{12})(CH_2O_2^{2-})(OH^-)]$. As was the case with polytungstate and polymolybdate structures based on different-sized $(M^{VI}O_3)_x$ cages formed from type **3** units described above, a large family of polymolybdate and polytungstate structures exists based on different-sized $(M^{VI}O_3)_x$ rings formed from type **7** units; $Mo_4O_{12}(O_2)_2^{4-}$ (*I*) contains two peroxide ions enclosed by an Mo_4O_{12} ring, $[(Mo_4O_{12})(O_2^{2-})_2]$; $S_2Mo_5O_{21}^{4-}$ (*I*) contains two sulfite ions enclosed by an Mo_5O_{15} ring, $[(Mo_5O_{15})(SO_3^{2-})_2]$; $C_6H_5AsMo_7O_{25}^{4-}$ (**9**) contains a molybdate ion and a phenylarsonate ion enclosed by an Mo_6O_{18} ring, $[(Mo_6O_{18})(MoO_4^{2-})(C_6H_5AsO_3^{2-})]$; $P_4W_8O_{40}^{12-}$ (*I*) contains four phosphate ions enclosed by a W_8O_{24} ring, $[(W_8O_{24})(PO_4^{3-})_4]$; and so on. In the limit of an infinitely large ring of units shown in **7**, one obtains an infinite chain structure. Precisely such chains are found in the MoO_3 structure (**10**). Within each chain, each molybdenum forms two double bonds to oxygen and two single bonds to oxygen. The two very weak molybdenum-

oxygen bonds formed at each molybdenum link these chains together; one is formed to an oxygen that has already formed two single bonds to other molybdenums, and the other is formed to an oxygen that has already formed a double bond to another molybdenum (10).

Multinuclear NMR Spectroscopy as a Structural Probe

All of the elements commonly found in early transition metal polyoxoanions, except tantalum, have nuclides suitable for NMR spectroscopy, and ^{51}V , ^{93}Nb , ^{95}Mo , and ^{183}W as well as ^{17}O have been used in NMR studies of polyoxoanion solution chemistry. Multinuclear NMR techniques have been available for decades, but their use on a routine basis became practical only with the recent commercial availability of high-resolution, high-sensitivity Fourier transform spectrometers operating at high magnetic fields. The examples discussed here, although restricted to ^{17}O NMR spectroscopy, illustrate the type of information that multinuclear NMR spectroscopy can provide.

The power of ^{17}O NMR spectroscopy as a structural probe

arises in large part from the high sensitivity of ^{17}O chemical shifts to environmental perturbations and the empirical relations that have been established between chemical shifts and structural environments. Derivatives of the $\text{W}_6\text{O}_{19}^{2-}$ anion provide good examples of how chemical shift data are interpreted and then used to help assign structures to incompletely characterized species. The ^{17}O NMR spectrum of $\text{W}_6\text{O}_{19}^{2-}$, shown in Fig. 1d, displays three resonances corresponding to its three structurally nonequivalent types of oxygen (11). Each of these resonances is uniquely assigned to a specific type of oxygen on the basis of its intensity; using the labeling scheme shown in Fig. 1a, resonance c is assigned to the six terminal OW oxygens (O_C), resonance b to the 12 doubly bridging OW_2 oxygens (O_B), and resonance a to the unique sixfold bridging OW_6 oxygen (O_A). The chemical shift values, given as high-frequency (low-field) shifts relative to pure water, conform to the general pattern observed for many other classes of oxygen compounds, where for a given element, stronger element-oxygen bonding, here stronger π bonding, yields larger chemical shift values (see 3 and 4) (11, 12).

The $[(\text{C}_5\text{H}_5)\text{Ti}(\text{W}_5\text{O}_{18})]^{3-}$ anion has been assigned a structure related to the $\text{W}_6\text{O}_{19}^{2-}$ ion by replacement of an

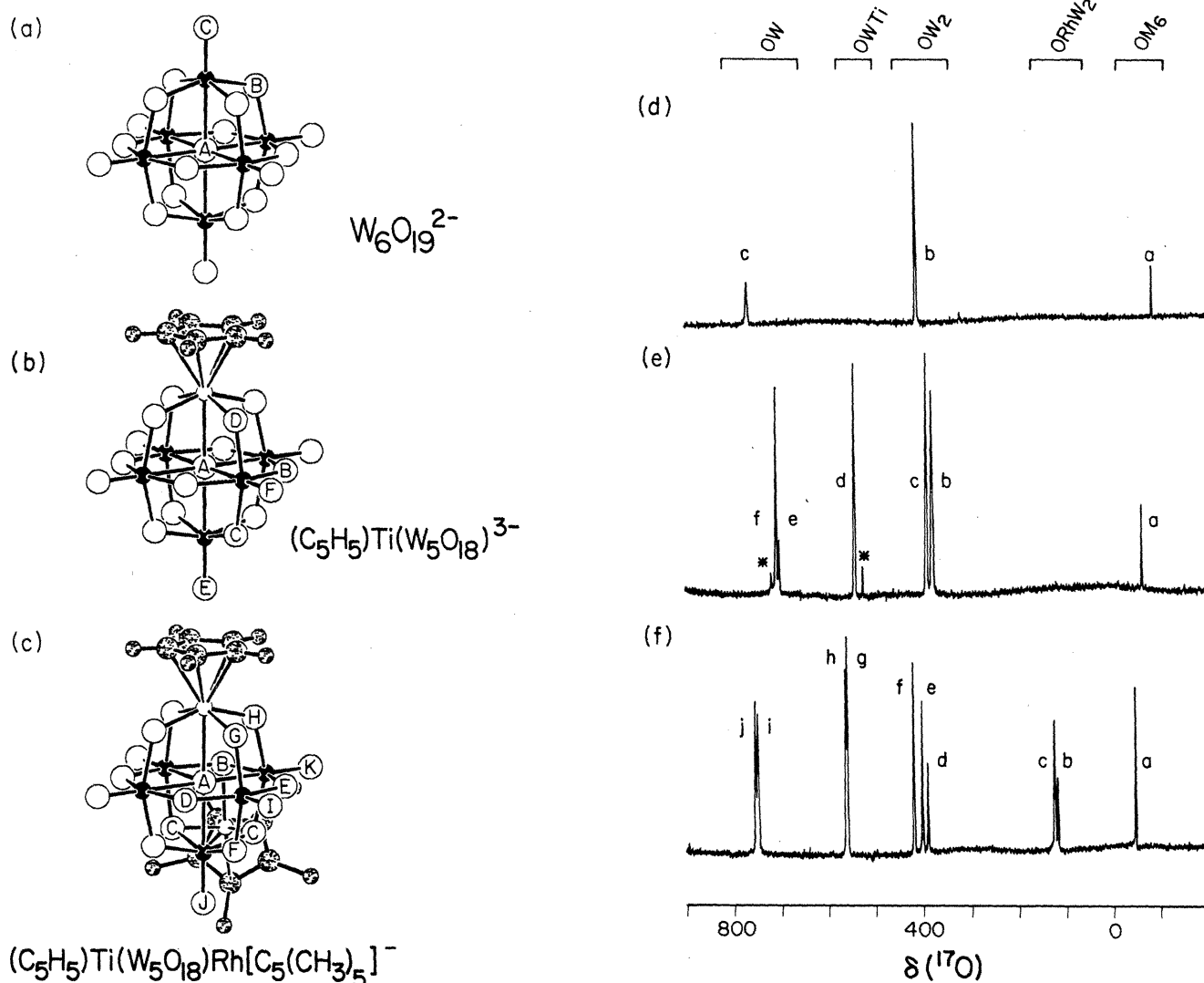


Fig. 1. Oxygen-17 NMR spectra of (a) $\text{W}_6\text{O}_{19}^{2-}$, (b) $(\text{C}_5\text{H}_5)\text{Ti}(\text{W}_5\text{O}_{18})^{3-}$, and (c) $(\text{C}_5\text{H}_5)\text{Ti}(\text{W}_5\text{O}_{18})\text{Rh}[\text{C}_5(\text{CH}_3)_5]^-$ as $(n\text{-C}_4\text{H}_9)_4\text{N}^+$ salts in CH_3CN are shown in (d), (e), and (f), respectively. In the structures, one member of each set of symmetry-equivalent oxygens is labeled with an uppercase letter. In the spectra, each resonance is labeled with a lowercase letter. Resonances labeled with a given letter (lowercase) are assigned, whenever possible, to oxygens labeled with the same letter (uppercase) in the corresponding structure, as described in the text.

[$\text{OW}^{\text{VI}}\text{]}^{4+}$ unit with a [$(\text{C}_5\text{H}_5)\text{Ti}^{\text{IV}}\text{]}^{3+}$ (see Fig. 1b) on the basis of the ^{17}O NMR spectrum shown in Fig. 1e (13, 14). Each of the resonances labeled a through f can be assigned to a type of oxygen in the proposed structure as follows. Resonances e and f are assigned to the OW oxygens since their chemical shift values are similar to those observed for OW oxygens in $\text{W}_6\text{O}_{19}^{2-}$. Resonances b and c are similarly assigned to the OW_2 oxygens and resonance a to the OW_5Ti oxygen by comparison with the OW_2 and OW_6 chemical shift values, respectively, for $\text{W}_6\text{O}_{19}^{2-}$. The remaining resonance, d, is then assigned by default to the OWTi oxygen. Note that there is a single ambiguity in the overall assignment scheme since the OW_2 resonances b and c in Fig. 1e cannot be uniquely assigned to the OW_2 oxygens B and C in Fig. 1b because they have equal intensities and very similar chemical shift values. However, the OW resonances, e and f, can be assigned to the OW oxygens labeled E and F, respectively, in Fig. 1b, since they have unequal intensities.

The final spectrum shown in Fig. 1, measured from a solution of the $[(\text{CH}_3)_5\text{C}_5\text{Rh}]^{2+}$ adduct of the $[(\text{C}_5\text{H}_5)\text{Ti}(\text{W}_5\text{O}_{18})]^{3-}$ ion, was used to propose the structure shown in Fig. 1c (14). Here, chemical shift data from $\text{W}_6\text{O}_{19}^{2-}$ and $[(\text{C}_5\text{H}_5)\text{Ti}(\text{W}_5\text{O}_{18})]^{3-}$ allow resonances in the OW, OWTi , OW_2 , and OW_5Ti regions to be assigned; the two ORhW_2 resonances are assigned by default. In contrast to the two spectra just discussed, this spectrum is not completely resolved: two resonances, i and j, are observed in the OW region, but the proposed structure contains three OW oxy-

gens, labeled I, J, and K in Fig. 1c. An important feature of the $\{(\text{C}_5\text{H}_5)\text{Ti}(\text{W}_5\text{O}_{18})\text{Rh}[(\text{C}_5\text{H}_5)_5\text{C}_5]^{-}$ spectrum is the location of the ORhW_2 resonances, displaced about 300 ppm upfield from the OW_2 chemical shift region. The transformation of doubly bridging OW_2 oxygens into triply bridging OW_2Rh oxygens implies a weakening of individual metal-oxygen bonds and consequently an upfield displacement of chemical shift values (15).

In the ^{17}O NMR spectra discussed thus far, spectral assignments have been made by using intensity arguments and chemical shift data from reference compounds. When these approaches fail, double-resonance heteronuclear decoupling experiments can sometimes be used to assign both oxygen and metal NMR spectra (16). The $\text{V}_{10}\text{O}_{28}^{6-}$ anion (see Fig. 2) is such a case. This anion contains three types of vanadium centers, two of type I and four each of types II and III. Only one of its ^{51}V NMR resonances, i in Fig. 2a, can therefore be assigned; the remaining two, ii and iii, arise from V_{II} and V_{III} and therefore have equal intensities. A similar situation prevails in the $\text{V}_{10}\text{O}_{28}^{6-}$ ^{17}O NMR spectrum (Fig. 2b). The resonances for the oxygens labeled A through E in Fig. 2 can be assigned by using bond-strength and intensity arguments (17), but the OV oxygens labeled F and G cannot be uniquely assigned to the two OV resonances labeled f and g in Fig. 2b. Since ^{17}O NMR resonances are broadened by spin-spin coupling to adjacent ^{51}V nuclei, ^{51}V decoupling of vanadium nuclei causes the ^{17}O NMR resonances of adjacent oxygen nuclei to sharpen. This is illustrated in Fig. 2, c through e.

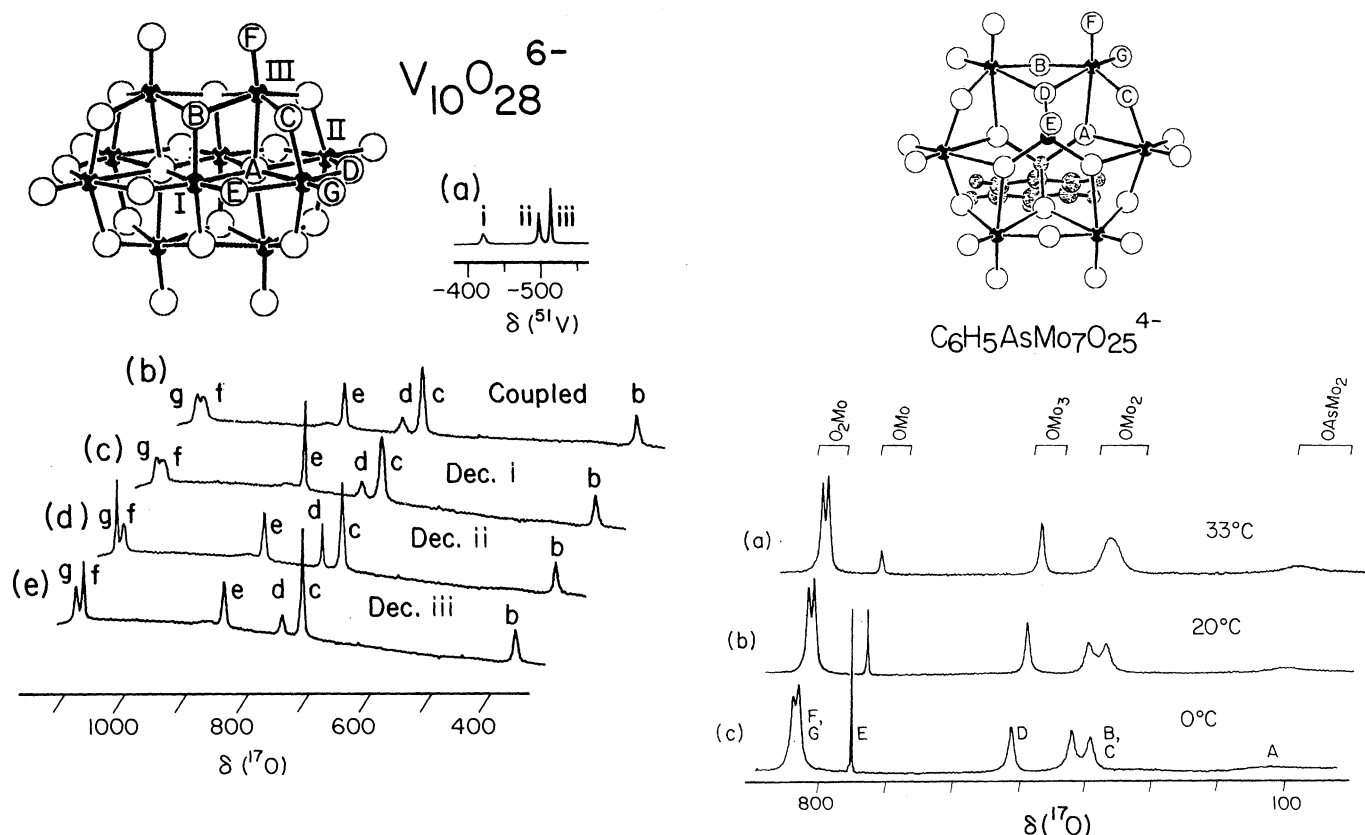


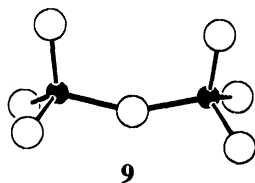
Fig. 2 (left). A drawing of the D_{2h} $\text{V}_{10}\text{O}_{28}^{6-}$ anion is shown at the top. One member of each set of symmetry-equivalent oxygen and vanadium atoms is labeled. The ^{51}V and ^{17}O NMR spectra shown in (a) through (e) were all measured from an aqueous $\text{Na}_6\text{V}_{10}\text{O}_{28}$ solution at 44°C. ^{17}O NMR spectra c through e were measured with decoupling of vanadium nuclei responsible for ^{51}V NMR resonances i through iii, respectively. Note that the water and OV_6 resonances are off the chemical shift range included in (b) through (e). Resonances labeled with a given letter or numeral (lowercase) are assigned to oxygens or metals labeled with the same letter or numeral (uppercase), as described in the text. Fig. 3 (right). Variable-temperature ^{17}O NMR spectra of $(\text{C}_6\text{H}_5\text{AsMo}_7\text{O}_{25})[(n\text{-C}_4\text{H}_9)_4\text{N}]_4$ in CH_3CN are shown in (a) through (c). In the anion structure, one member of each set of symmetry-equivalent oxygen atoms is labeled, assuming free rotation of the C_6H_5 group about its C-As bond.

Sample irradiation at the frequency of ^{51}V resonance ii (see Fig. 2d), for example, sharpens ^{17}O resonances d and g markedly. Since ^{17}O resonance d is assigned to oxygen D, and oxygen D is bonded to V_{II} only, ^{51}V resonance ii must be assigned to V_{II} . Since O_{G} is bonded to V_{II} , ^{17}O resonance g must be assigned to O_{G} . Using heteronuclear decoupling experiments, one can in this fashion provide unique assignments for all the ^{51}V and ^{17}O resonances observed in NMR spectra of the $\text{V}_{10}\text{O}_{28}^{6-}$ anion (16).

Solution dynamics can also be probed with ^{17}O NMR spectroscopy. In the absence of chemical exchange processes, ^{17}O NMR resonances narrow with increasing temperature as quadrupolar relaxation rates diminish. The opposite effect is observed for resonances of oxygens involved in chemical exchange processes. Their resonances broaden with increasing temperature as the chemical exchange rate increases, thus lowering the lifetimes of nuclei in a given chemical environment. Consider the spectra of the $\text{C}_6\text{H}_5\text{AsMo}_7\text{O}_{25}^{4-}$ ion shown in Fig. 3 (9). Here, the resonances assigned to oxygens A, F, and G narrow with increasing temperature while the resonances labeled B, C, D, and E broaden. The OMo_2 , OMo_3 , and OMo oxygens are therefore involved in a chemical exchange process, but since exchange narrowing effects are superimposed upon quadrupolar broadening effects, differential line narrowing cannot be interpreted to obtain mechanistic information. Spin saturation transfer experiments are able to show, however, that two separate exchange processes are responsible for the observed line shape behavior; one involves exchange between O_{B} and O_{C} oxygens, the other between O_{D} and O_{E} oxygens (9). If one formulates the $\text{C}_6\text{H}_5\text{AsMo}_7\text{O}_{25}^{4-}$ anion in terms of its subunits as described above, $[(\text{Mo}_6\text{O}_{18})\text{-(MoO}_4^{2-})(\text{C}_6\text{H}_5\text{AsO}_3^{2-})]$, the former process corresponds to inversion of the Mo_6O_{18} ring subunit, and the latter process corresponds to reorientation of the tetrahedral MoO_4^{2-} subunit. Crossover labeling experiments show that this reorientation occurs in an intramolecular fashion, and a detailed mechanism has been proposed which accounts for the observed rapid site exchanges by breaking and reforming only the very weak bonds that interconnect the three $\text{C}_6\text{H}_5\text{AsMo}_7\text{O}_{25}^{4-}$ subunits (9).

Organic and Organotransition Metal Chemistry

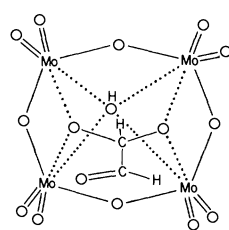
The range of chemical reactivity displayed by polyoxoanions in aprotic environments is nicely illustrated by the chemistry of the $\text{Mo}_2\text{O}_7^{2-}$ ion, 9, which is quite soluble in several organic solvents as a $(n\text{-C}_4\text{H}_9)_4\text{N}^+$ salt (18). To



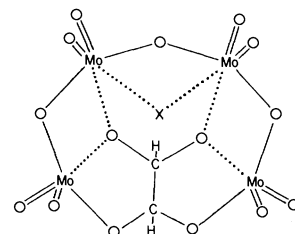
emphasize the contrast between its nonaqueous chemistry and aqueous acid-base chemistry, it should be pointed out that the dimolybdate ion reacts with water to form the $\text{Mo}_5\text{O}_{17}\text{H}^{3-}$ ion (19). This species is related to the $\text{CH}_2\text{Mo}_4\text{O}_{15}\text{H}^{3-}$ anion (see 5) by replacement of a tetrahedral $\text{CH}_2\text{O}_2^{2-}$ unit with a tetrahedral MoO_4^{2-} unit and can thus be formulated $[(\text{Mo}_4\text{O}_{12})(\text{MoO}_4^{2-})(\text{OH}^-)]$.

The $\text{Mo}_2\text{O}_7^{2-}$ ion reacts with hydrated aldehydes RCHO ($\text{R} = \text{H}, \text{CH}_3, \text{CHCH}_2, \text{C}_6\text{H}_5, \text{and CF}_3$) to form adducts $\text{RCHMo}_4\text{O}_{15}\text{H}^{3-}$ (8). These derivatives have a common struc-

ture described above for the $\text{R} = \text{H}$ case (see 5, 6, and 8). Since this structure places the R group in close proximity to an OMo_2 bridging oxygen, it provides a good opportunity for studying interactions between organic functional groups and metal-oxygen frameworks. The aldehyde group, for example, is incorporated into the $\text{RCHMo}_4\text{O}_{15}\text{H}^{3-}$ structure (see 10) by reacting $\text{Mo}_2\text{O}_7^{2-}$ with glyoxal, OHCCHO . The carbonyl

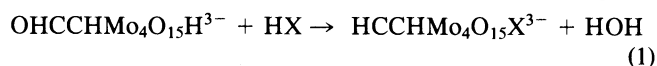


10



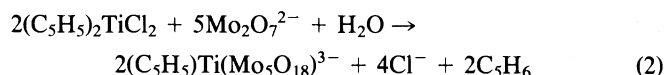
11

($\text{C}=\text{O}$) group in 10 inserts into an adjacent $\text{Mo}-\text{O}$ bond when the fourfold bridging OH^- group in the structure is replaced by a doubly bridging X^- group (see 11) according to Eq. 1

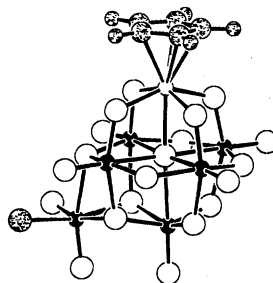


where $\text{X} = \text{HCOO}$ or F . A remarkable feature of these product anions is the manner in which anions X^- of such different sizes are accommodated into the $\text{HCCHMo}_4\text{O}_{15}\text{X}^{3-}$ structure. Comparison of the structures of the F^- and HCOO^- adducts in Fig. 4 shows how the necessary conformational flexibility is achieved, largely through variation of the $\text{Mo}_2\text{-O}_{\text{F}}\text{-Mo}_2'$ angle, which determines the $\text{Mo}_2 \cdot \cdot \text{Mo}_2'$ separation, and rotation about the carbon-carbon bond, which varies the $\text{Mo}_1 \cdot \cdot \text{Mo}_1'$ separation.

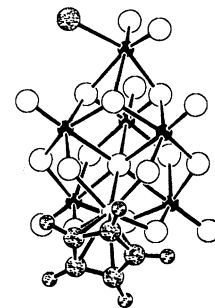
The $\text{Mo}_2\text{O}_7^{2-}$ ion also provides an entry into organotransition metal derivative chemistry. Reaction with $(\text{C}_5\text{H}_5)_2\text{TiCl}_2$ and water according to Eq. 2



yields a product isostructural with the $(\text{C}_5\text{H}_5)_3\text{Ti}(\text{W}_5\text{O}_{18})^{3-}$ anion shown in Fig. 1b (20). The water-sensitive $(\text{C}_5\text{H}_5)_3\text{Ti}(\text{Mo}_5\text{O}_{18})^{3-}$ anion itself has an interesting reaction chemistry. Upon reaction with HCl , the $(\text{C}_5\text{H}_5)_3\text{Ti}(\text{Mo}_6\text{O}_{20}\text{Cl})^{2-}$ anion is formed (21). The structural representation 12 shows it to be an MoO_2Cl^+ adduct of the reactant. Viewed from another perspective, 13, the adduct chlorine and oxygen atoms



12

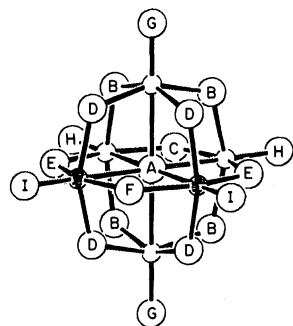


13

seen to extend the cubic close-packed oxygen array of the $(\text{C}_5\text{H}_5)_3\text{Ti}(\text{Mo}_5\text{O}_{18})^{3-}$ unit (see 1 and 2). Analogous $(\text{OC})_3\text{Mn}^+$ and $[(\text{CH}_3)_5\text{C}_5]\text{Rh}^{2+}$ adducts are obtained by simply reacting $(\text{C}_5\text{H}_5)_3\text{Ti}(\text{Mo}_5\text{O}_{18})^{3-}$ with the solvated cations $(\text{OC})_3\text{Mn}(\text{NCCH}_3)_3^+$ and $[(\text{CH}_3)_5\text{C}_5]\text{Rh}(\text{NCCH}_3)_3^{2+}$, respectively (14, 21). These organometallic units bind to the same $(\text{C}_5\text{H}_5)_3\text{Ti}$ -

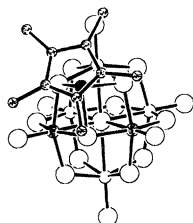
(Mo₅O₁₈)³⁻ oxygens bonded to the MoO₂Cl⁺ metal center in **12** and **13**.

The Mo₂O₇²⁻ ion illustrates the remarkable structural transformations which polyoxoanions may undergo upon reaction with organic and organometallic units. The *cis*-Nb₂W₄O₁₉⁴⁻ anion, **14**, is also soluble in polar organic solvents and reactive

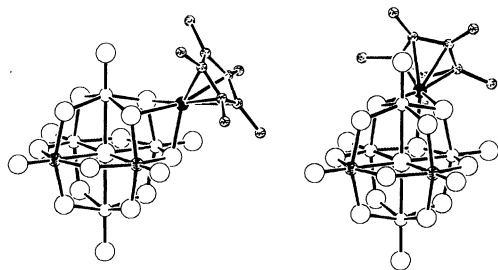


14

toward a number of organic and organometallic reagents, but displays a quite different type of behavior. It has a far more rigid metal-oxygen framework and is frequently able to form adducts without losing its structural integrity. A few examples of its reaction chemistry should suffice to show the variety of derivatives which can be prepared. Reaction of the *cis*-Nb₂W₄O₁₉⁴⁻ ion with (CH₃)₂SO₄ yields Nb₂W₄O₁₉CH₃³⁻ as a mixture of the five isomers resulting from methylation of the five nonequivalent doubly bridging oxygens in *cis*-Nb₂W₄O₁₉⁴⁻, labeled F, D, E, B, and C in **14** (22). Silylation with (CH₃)₃SiCl/[(CH₃)₃Si]₂NH, on the other hand, yields Nb₂W₄O₁₉Si(CH₃)₃³⁻ exclusively as the isomer resulting from silylation at the ONb oxygen labeled I in **14** (22). Organotransition metal adducts also show structural diversity. When the *cis*-Nb₂W₄O₁₉⁴⁻ ion reacts with [(CH₃)₅C₅]Rh(NCCH₃)₃²⁺, three diastereomeric [(CH₃)₅C₅]Rh(Nb₂W₄O₁₉)²⁻ anions, **15**, **16**, and **17**, are formed, corresponding to the three ways in



15

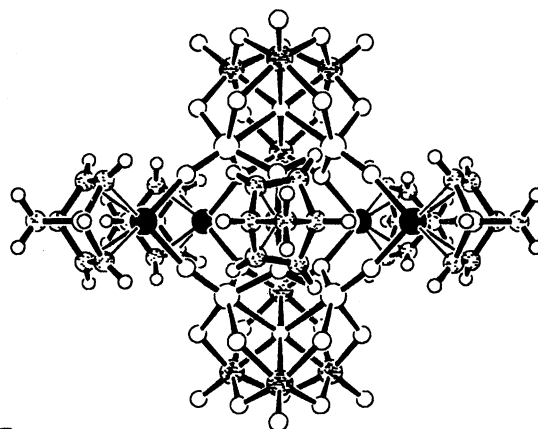


16

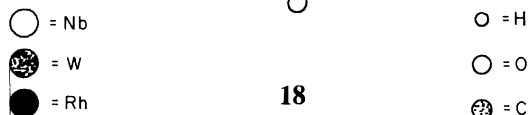
17

which [(CH₃)₅C₅]Rh²⁺ can bind to a triangle of three *cis*-Nb₂W₄O₁₉⁴⁻ bridging oxygens (23). An analogous set of three diastereomeric (OC)₃M(Nb₂W₄O₁₉)³⁻ anions is formed from *cis*-Nb₂W₄O₁₉⁴⁻ and (OC)₃M(NCCH₃)₃⁺, M = Mn or Re, where the (OC)₃M unit is bound to three polyoxoanion oxygens (24, 25). Although norbornadienerhodium(I) could form similar adducts by forming three rhodium-oxygen bonds

as it does in (C₇H₈)Rh(P₃O₉)²⁻, it behaves quite differently in the reaction between (C₇H₈)Rh(NCCH₃)₂⁺ and *cis*-Nb₂W₄O₁₉⁴⁻, forming the 5:2 adduct [(C₇H₈)Rh]₅(Nb₂W₄O₁₉)₂³⁻ as the single isomer shown in **18** (26). Here, each Rh^I center is bonded to only two oxygens, and both ONb₂ and ONbW bridging oxygens as well as ONb terminal oxygens in *cis*-Nb₂W₄O₁₉⁴⁻ are used as rhodium binding sites.

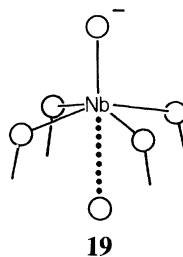


18

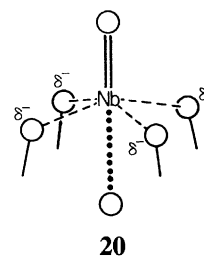


Structure, Bonding, Reactivity, and Mechanism

Given all the detailed information presented thus far, it is natural to ask whether patterns of chemical behavior have been observed which relate polyoxoanion structure, bonding, and reactivity. Since polyoxoanion reaction chemistry can become predictable and hence controllable only when mechanistic pathways become predictable, and since mechanistic predictions must be based on structure-reactivity correlations, the problem of relating polyoxoanion structure, bonding, reactivity, and reaction mechanism is of paramount importance. Most research addressing this problem has focused on the chemistry of polyoxoanions closely related to the W₆O₁₉²⁻ anion introduced above, specifically the (C₅H₅)Ti(M₅O₁₉)³⁻ (M = Mo and W) and *cis*-Nb₂W₄O₁₉⁴⁻ anions. The W₆O₁₉²⁻ ion is very nonbasic, less basic than the ClO₄⁻ ion according to heteroconjugation studies (27), and hence unreactive in solution at ambient temperature toward many good electrophiles such as (CH₃)₂SO₄ and (OC)₃Mn(NCCH₃)₃⁺. This low reactivity is easily understood in terms of bonding scheme **4** introduced above. The OW and OW₂ oxygens which form the surface of the anion all have their divalence satisfied, whereas the potentially reactive OW₆ oxygen, which is only weakly bound to tungsten centers, is shielded from the anion's environment by the surrounding W₆O₁₈ cage. One approach to the activation of W₆O₁₉²⁻ surface oxygens involves replacement of W^{VI} centers with lower-valent d⁰ centers such as Nb^V. The resonance forms **19** and **20** show two extreme



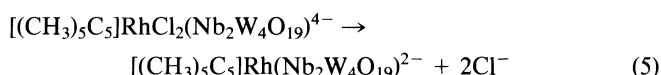
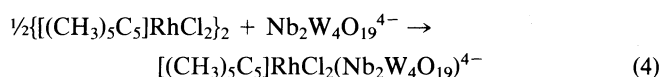
19



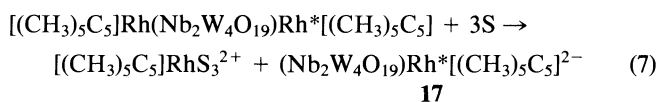
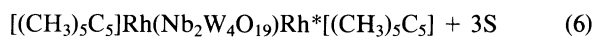
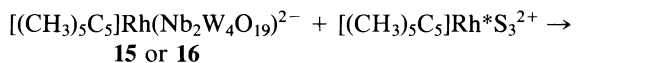
20

processes. Consider, for example, the reaction between $\{[(\text{CH}_3)_5\text{C}_5]\text{RhCl}_2\}_2$ and $\text{cis-Nb}_2\text{W}_4\text{O}_{19}^{4-}$ which results in displacement of Cl^- ions from the rhodium complex and formation of $[(\text{CH}_3)_5\text{C}_5]\text{Rh}(\text{Nb}_2\text{W}_4\text{O}_{19})^{2-}$ as a mixture of only two diastereomers, **15** and **16**, according to ^1H and ^{17}O NMR spectroscopy (23). This result contrasts with the case mentioned above where $[(\text{CH}_3)_5\text{C}_5]\text{Rh}(\text{NCCH}_3)_3^{2+}$ reacts with $\text{cis-Nb}_2\text{W}_4\text{O}_{19}^{4-}$ to form the same product as a three-diastereomer mixture (**15**, **16**, and **17**). Since the mixture of **15** and **16** is converted rapidly to the mixture of **15**, **16**, and **17** in the presence of catalytic amounts of solvated $[(\text{CH}_3)_5\text{C}_5]\text{Rh}^{2+}$ (23), the three-diastereomer mixture is the equilibrium product distribution. The $[(\text{CH}_3)_5\text{C}_5]\text{Rh}(\text{Nb}_2\text{W}_4\text{O}_{19})^{2-}$ system thus poses two mechanistic questions: How does $\{[(\text{CH}_3)_5\text{C}_5]\text{RhCl}_2\}_2$ react to form only diastereomers **15** and **16**, and how are these diastereomers converted to **17** (28)?

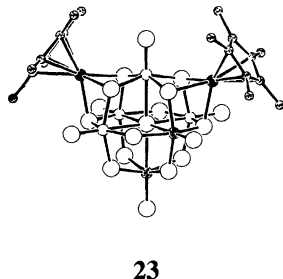
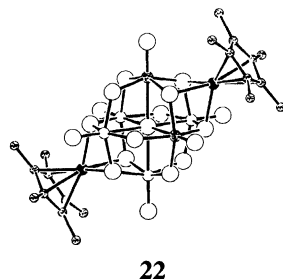
The first mechanistic question just raised, that concerning the formation of $[(\text{CH}_3)_5\text{C}_5]\text{Rh}(\text{Nb}_2\text{W}_4\text{O}_{19})^{2-}$ as a two-diastereomer mixture, is resolved by the following two-step mechanism:



In the product of reaction 4, the $[(\text{CH}_3)_5\text{C}_5]\text{RhCl}_2$ unit is linked to $\text{Nb}_2\text{W}_4\text{O}_{19}^{4-}$ ion by a single Rh–O bond, and because the Rh center is sterically congested this linkage occurs exclusively at the ONb oxygen site (O_I in **14**). In the second step, the Rh– O_I and Rh–Cl bonds are cleaved and three new Rh–O bonds are formed to adjacent ONb₂, ONbW, and OW_2 oxygens, yielding product diastereomers **15** and **16**. The reason why **17** is not formed is now clear: the rhodium binding site in **17**, two O_B oxygens and one O_C oxygen in **14**, is not adjacent to an ONb oxygen and thus not accessible. The isomerization of **15** and **16** into **17** catalyzed by $\{[(\text{CH}_3)_5\text{C}_5]\text{Rh}(\text{S})_3\}^{2+}$, S = solvent, can also be understood in terms of a two-step mechanism:



Possible intermediates in the transformations of **15** to **17** and **16** to **17** are shown in **22** and **23**, respectively. A key property of the catalyst is its ability to weaken Rh–O bonds in the reactant isomer by formation of a dirhodium adduct. Formation of Rh*–O bonds weakens Rh–O bonds through a series of bond length alternations similar to those discussed above.



This type of bond length alternation, induced by cation binding, has been characterized in detail in an x-ray crystallographic study of the MoO_2Cl^+ adduct of the $(\text{C}_5\text{H}_5)\text{Ti}(\text{Mo}_5\text{O}_{18})^{3-}$ anion (21).

Outlook

The research efforts just described, performed largely in the authors' laboratories, have been concerned with understanding and controlling the structure and reactivity of very simple polyoxoanions under very simple reaction conditions, thus laying the foundation for understanding larger, more complex systems. These larger systems, under active investigation in several laboratories, are already bridging the gap between the solution chemistry of polyoxoanions and the solid-state chemistry of metal oxide lattice compounds. Several research groups in the United States at Georgetown University [for example, (29)], DuPont Central Research (30), and the University of Oregon (31); in France at the Université Pierre et Marie Curie (32) and the Université des Sciences et Techniques du Languedoc (33); in Japan at the University of Tokyo (34); in the Soviet Union at the Moscow Institute of Physical Chemistry and the Novosibirsk Institute of Catalysis (35); and in Germany at the Berlin Free University (36), have been preparing and characterizing species of increasingly massive size, such as the recently reported $\text{P}_8\text{W}_{48}\text{O}_{184}^{40-}$ anion (37). Other researchers are exploring the photochemical behavior of early transition metal polyoxoanions and its relationship to photochemistry on semiconductor oxide surfaces (38). A similar approach is apparent in recent studies of organic polyoxoanion derivatives, where parallels with solid oxide surface chemistry are being examined (39). Finally, the reaction chemistry of polyoxoanions toward small covalent molecules in the solid state is being studied by Misono (4) and others, merging the solution chemistry of large polyoxoanions with the solid-state chemistry of metal oxides to create what has been designated a "pseudo-liquid phase."

References and Notes

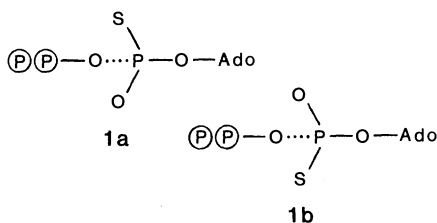
- M. T. Pope, *Heteropoly and Isopoly Oxometalates* (Springer-Verlag, Heidelberg, 1983).
- P. Souchay, *Ions Minéraux Condenses* (Masson, Paris, 1969).
- A. Rosenheim and R. Bilecki, *Chem. Ber.* **46**, 539 (1913).
- M. Misono, in *Proceedings of the Climax Fourth International Conference of the Chemistry and Uses of Molybdenum*, H. F. Barry and P. C. H. Mitchell, Eds. (Climax Molybdenum Company, Ann Arbor, Mich., 1982), pp. 289–295.
- J. Fuchs, W. Freiwald, H. Hartl, *Acta Crystallogr. Sect. B.* **34**, 1764 (1978).
- The terms "double bond" and "single bond" refer not to bond order (orbital components) but to bond strength in the classical, electrostatic sense. See (1).
- B. Krebs, *Acta Crystallogr. Sect. B.* **28**, 2222 (1972).
- V. W. Day, M. F. Fredrich, W. G. Klemperer, R.-S. Liu, *J. Am. Chem. Soc.* **101**, 491 (1979).
- W. G. Klemperer, C. Schwartz, D. A. Wright, in preparation.
- L. Kihlberg, *Ark. Kemi* **21**, 357 (1963).
- M. Filowitz, R. K. C. Ho, W. G. Klemperer, W. Shum, *Inorg. Chem.* **18**, 93 (1979).
- W. G. Klemperer, *Angew. Chem. Int. Ed. Engl.* **17**, 246 (1978).
- , in *The Multinuclear Approach to NMR Spectroscopy*, J. B. Lambert and F. G. Riddell, Eds. (Reidel, Dordrecht, 1983), pp. 245–260.
- T. M. Che, V. W. Day, L. C. Francesconi, M. F. Fredrich, W. G. Klemperer, W. Shum, *Inorg. Chem.*, in press.
- W. G. Klemperer and W. Shum, *J. Am. Chem. Soc.* **100**, 4891 (1978).
- C. J. Besecker, W. G. Klemperer, D. J. Maltbie, D. A. Wright, *Inorg. Chem.* **24**, 1027 (1985).
- W. G. Klemperer and W. Shum, *J. Am. Chem. Soc.* **99**, 3544 (1977).
- V. W. Day, M. F. Fredrich, W. G. Klemperer, W. Shum, *ibid.*, p. 6146.
- M. Filowitz, W. G. Klemperer, W. Shum, *ibid.* **100**, 2580 (1978).
- W. G. Klemperer and W. Shum, *J. Chem. Soc. Chem. Commun.* (1979), p. 60.
- V. W. Day, M. F. Fredrich, M. R. Thompson, W. G. Klemperer, R.-S. Liu, W. Shum, *J. Am. Chem. Soc.* **103**, 3597 (1981).
- V. W. Day, W. G. Klemperer, C. Schwartz, in preparation.
- C. J. Besecker, V. W. Day, W. G. Klemperer, M. R. Thompson, *J. Am. Chem. Soc.* **106**, 4125 (1984).
- C. J. Besecker and W. G. Klemperer, *ibid.* **102**, 7598 (1980).
- C. J. Besecker, V. W. Day, W. G. Klemperer, M. R. Thompson, *Inorg. Chem.* **24**, 44 (1985).

26. C. J. Besecker, W. G. Klemperer, V. W. Day, *J. Am. Chem. Soc.* **104**, 6158 (1982).
27. The $\text{Mo}_6\text{O}_{19}^{2-}$ ion is less basic than ClO_4^- , and tungstates are less basic than isostructural molybdates [L. Barcza and M. T. Pope, *J. Phys. Chem.* **79**, 92 (1975)].
28. For a very detailed discussion, see (23).
29. S. P. Harmaker, M. A. Lelparulo, M. T. Pope, *J. Am. Chem. Soc.* **105**, 4286 (1983); R. Acerete, C. F. Hammer, L. C. W. Baker, *ibid.* **104**, 5384 (1982).
30. P. J. Dmaille and W. H. Knoth, *Inorg. Chem.* **22**, 818 (1983); E. M. McCarron III, J. F. Whitney, D. B. Chase, *ibid.* **23**, 3275 (1984).
31. R. G. Finke and M. W. Droegge, *ibid.* **22**, 1007 (1983).
32. C. Sanchez, J. Livage, J. P. Launay, M. Fournier, Y. Jeannin, *J. Am. Chem. Soc.* **104**, 3194 (1982); F. Robert, M. Leyrie, G. Herve, *Acta Crystallogr. Sect. B* **38**, 358 (1982).
33. C. Brevard, R. Schimpf, G. Tourné, C. M. Tourné, *J. Am. Chem. Soc.* **105**, 7059 (1983).
34. U. Lee, A. Kobayashi, Y. Sasaki, *Acta Crystallogr. Sec. C* **39**, 817 (1983).
35. L. P. Kazansky and M. A. Fedotov, *J. Chem. Soc. Chem. Commun.* (1983), p. 417.
36. J. Fuchs and E.-P. Flindt, *Z. Naturforsch. Teil B* **34**, 412 (1979).
37. A. Tézé, paper presented at the United States-France Workshop on the Synthesis, Structure, and Reactivity of Polyoxoanions, St. Lambert des Bois, France, August 1983.
38. T. Yamase and R. Watanabe, *Inorg. Chim. Acta* **77**, L193 (1983); E. Papaconstantinou, *J. Chem. Soc. Chem. Commun.* (1982), p. 12; J. R. Darwent, *ibid.* (1982), p. 798.
39. E. M. McCarron and R. L. Harlow I, *J. Am. Chem. Soc.* **105**, 6179 (1983).
40. We gratefully acknowledge contributions from our co-workers M. Filowitz, W. Shum, M. F. Fredrich, R. K. C. Ho, G. Rupprecht, R.-S. Liu, M. R. Thompson, C. S. Day, C. J. Besecker, T. Che, L. C. Francesconi, D. J. Maltbie, and C. Schwartz. We are also grateful to E. Keller for providing a copy of his SCHAKAL program.

Bond Order and Charge Localization in Nucleoside Phosphorothioates

Perry A. Frey and R. Douglas Sammons

Sulfur-containing analogs of biological phosphoric esters and phosphoanhydrides are widely used as substrate analogs in studies of enzymatic processes. Substitution of sulfur for one of the diastereotopic oxygens at P_α of ATP generates epimers **1a** and **1b** of $\text{ATP}_\alpha\text{S}$ (*1*),



differing in configuration at phosphorus (2, 3). Similar substitution at P_β of ATP or the phosphodiester group of 3',5'-cyclic AMP results in similar epimer pairs (2, 4-6). These compounds have been widely used as substrates or substrate analogs to determine the stereochemical course of enzymatic substitution at phosphorus (7). Both $\text{ATP}_\alpha\text{S}$ and ATP_βS have been used with divalent metal ions such as Mg^{2+} , Cd^{2+} , and Co^{2+} to determine the coordination structures and stereochemical configurations of active $\text{Me} \cdot \text{ATP}$ and $\text{Me} \cdot \text{ADP}$ complexes at the active sites of enzymes (7-10).

Epimer pairs such as **1a** and **1b** show

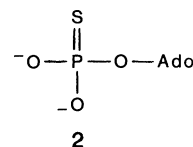
Perry A. Frey is a professor in the Institute for Enzyme Research and Professor of Biochemistry at the University of Wisconsin, Madison 53705. R. Douglas Sammons is a senior research chemist, Monsanto Agricultural Products Company, St. Louis, Missouri 16801.

varying degrees of stereoselectivity in their interactions with enzymes. In cases in which the chiral phosphorothioate group is the reaction center—that is, a bond in this group is cleaved—enzymes are very highly stereoselective or even stereospecific in their acceptance of only one epimer as a substrate. An interesting specific example of stereoselectivity is the dual interaction of valyl-tRNA synthetase with $(R_p)\text{-ATP}_\beta\text{S}$ and $(S_p)\text{-ATP}_\beta\text{S}$. The enzyme utilizes only the (R_p) epimer as an aminoacylation substrate but also catalyzes the interconversion of $(S_p)\text{-ATP}_\beta\text{S}$ and $\text{ATP}_\gamma\text{S}$ (*11*). The two processes apparently occur at different sites since neither epimer inhibits the reaction of the other.

Functional selectivity extends to interactions at allosteric sites, as in the activation of cyclic AMP-dependent protein kinases by (S_p) -cyclic AMPS (*12-14*). The (R_p) epimer is bound by the regulatory subunit but does not induce its dissociation from the catalytic subunit. Failure to induce dissociation and activation has been attributed to the absence of an electrostatic or hydrogen bond interaction between the regulatory subunit and the phosphorothioate group in (R_p) -cyclic AMPS. This interaction with cyclic AMP or (S_p) -cyclic AMPS is postulated to touch off a conformational transition in the regulatory subunit and stabilize the new conformation. This presumably weakens subunit interactions between the regulatory and catalytic subunits,

leading to their dissociation and the expression of protein kinase activity by the catalytic subunit.

The nature of the differential interactions between a binding site and ligand isomers can give important information about the molecular basis for function when one isomer is functional and the other not. In considering the possibilities for interactions between a nucleotide binding site and epimer pairs such as (R_p) -cyclic AMPS and (S_p) -cyclic AMPS or $(R_p)\text{-ATP}_\beta\text{S}$ and $(S_p)\text{-ATP}_\beta\text{S}$, it is essential to know as much as possible about the structures of the phosphorothioate groups. Structural formulas such as **1a** and **1b** for $(R_p)\text{-ATP}_\alpha\text{S}$ and $(S_p)\text{-ATP}_\alpha\text{S}$ illustrate only the steric differences between epimers, not the electronic and electrostatic differences. Structural formulas intended to emphasize localization of negative charges and double bonds are frequently shown with a double bond between the phosphorus and sulfur as in AMPS, **2**, below (7, 9, 15-17). These structures are intended to indicate that the negative electrostatic charges are localized on oxygen, with little resonance delocalization to sulfur.



In this article we review the experimental evidence bearing on the question of charge localization and bond order in phosphorothioate anions and point out that the evidence is not consistent with localization of charge on oxygen or with a bond order of 2 for the P-S bond.

P-O and P-S bond lengths. The crystal and molecular structure of *endo*-2'-3'-cyclic UMPS **3** was published by

